



HAL
open science

Camelid-derived T cell engagers harnessing human $\gamma\delta$ T cells as promising antitumor immunotherapeutic agents

Lola Boutin, Clement Barjon, Morgane Chauvet, Laura Lafrance, Eric Senechal, Dorothée Bourges, Emmanuelle Vigne, Emmanuel Scotet

► To cite this version:

Lola Boutin, Clement Barjon, Morgane Chauvet, Laura Lafrance, Eric Senechal, et al.. Camelid-derived T cell engagers harnessing human $\gamma\delta$ T cells as promising antitumor immunotherapeutic agents. *European Journal of Immunology*, inPress, 10.1002/eji.202350773 . hal-04591412

HAL Id: hal-04591412

<https://hal.science/hal-04591412v1>




Submitted on 28 May 2024

HAL is a multi-disciplinary open access archive for the deposit and dissemination of scientific research documents, whether they are published or not. The documents may come from teaching and research institutions in France or abroad, or from public or private research centers.

L'archive ouverte pluridisciplinaire **HAL**, est destinée au dépôt et à la diffusion de documents scientifiques de niveau recherche, publiés ou non, émanant des établissements d'enseignement et de recherche français ou étrangers, des laboratoires publics ou privés.

Research Article

Camelid-derived T cell engagers harnessing human $\gamma\delta$ T cells as promising antitumor immunotherapeutic agents

Lola Boutin^{1,2,3} , Clément Barjon⁴, Morgane Chauvet^{1,2,4},
Laura Lafrance^{1,2}, Eric Senechal³, Dorothee Bourges⁴,
Emmanuelle Vigne³  and Emmanuel Scotet^{1,2} 

¹ Nantes Université, Inserm UMR 1307, CNRS UMR 6075, Université d'AngersCRCI2NA, Nantes, France

² LabEx IGO "Immunotherapy, Graft, Oncology", Nantes, France

³ Sanofi, Large Molecule Research, Vitry-sur-Seine, France

⁴ Sanofi, Oncology, Vitry-sur-Seine, France

In the last decade, there has been a surge in developing immunotherapies to enhance the immune system's ability to eliminate tumor cells. Bispecific antibodies known as T cell engagers (TCEs) present an attractive strategy in this pursuit. TCEs aim to guide cytotoxic T cells toward tumor cells, thereby inducing a strong activation and subsequent tumor cell lysis. In this study, we investigated the activity of different TCEs on both conventional alpha-beta ($\alpha\beta$) T cells and unconventional gamma delta ($\gamma\delta$) T cells. TCEs were built using camelid single-domain antibodies (VHHs) targeting the tumor-associated antigen CEA-CAM5 (CEA), together with T cell receptor chains or a CD3 domain. We show that V γ 9V δ 2 T cells display stronger *in vitro* antitumor activity than $\alpha\beta$ T cells when stimulated with a CD3xCEA TCE. Furthermore, restricting the activation of fresh human peripheral T cells to V γ 9V δ 2 T cells limited the production of protumor factors and proinflammatory cytokines, commonly associated with toxicity in patients. Taken together, our findings provide further insights that $\gamma\delta$ T cell-specific TCEs hold promise as specific, effective, and potentially safe molecules to improve antitumor immunotherapies.

Keywords: activation · cancer · immunotherapy · T cell engager · $\gamma\delta$ T lymphocyte



Additional supporting information may be found online in the Supporting Information section at the end of the article.

Introduction

Over the last decade, redirecting immune cells against tumor cells using bispecific antibodies has been investigated as a promising and attractive strategy among antitumor immunotherapies. T cell

engagers (TCEs) are bispecific molecules designed to bind both T cells via T cell receptors (TCRs) and target cells via specifically expressed antigens [1]. Simultaneous binding to the two types of cells induces the formation of an active immune synapse and leads to the death of the target cell without the need for costimulatory signals [2–4] while bypassing tumor escape mechanisms such as major histocompatibility complex (MHC) downregulation. These molecules can be primarily classified according to the presence, or the absence, of an Fc region, the number of binding sites,

Correspondence: Dr. Emmanuelle Vigne and Dr. Emmanuel Scotet
e-mail: Emmanuelle.Vigne@sanofi.com; Emmanuel.Scotet@univ-nantes.fr

and overall geometry, which together govern their pharmacokinetic and pharmacodynamic properties [5]. Their antigen-binding sites may arise from conventional two-chain immunoglobulins or from single-domain antibodies (sdAb), also called VHHs (Variable Heavy domain of Heavy chain-only antibody), of camelid origin [6–8]. VHHs are modular building blocks characterized by their small size (15 kDa) and excellent biophysical properties, which enable their easy assembly into multi-specific functional molecules. They are well suited for therapy, as proven by the recent approval in Japan of Ozoralizumab, a trivalent anti-TNF- α Nanobody compound, for the treatment of rheumatoid arthritis [9].

Initial studies highlighted a therapeutic benefit of TCEs in the treatment of hematological malignancies, leading to the approval of Blinatumomab (CD3xCD19) or Mosunetuzumab (CD3xCD20) in the treatment of acute lymphoblastic B-cell leukemia and follicular lymphoma, respectively [10, 11]. More recently, clinical trials using TCEs targeting the prostate-specific membrane antigen (PSMA) or human epidermal growth factor receptor 2 have reported promising results in solid tumors [12, 13]. A recent study has further demonstrated the benefits of combining TCE therapy with immune checkpoint blockade (ICB) and a 4-1BB agonist in T cell cold solid tumors, where ICB monotherapy did not show any therapeutical benefit [14, 15].

The majority of current TCEs target T cells via the CD3 signaling complex, thus inducing strong polyclonal T cell activation. TCEs were initially designed to trigger minimal side effects by promoting tumor site-specific T cell recruitment, infiltration, and activation. However, stage 3 (or higher) deleterious effects in patients, such as cytokine release syndrome (CRS), neurotoxicity, and neutropenia, are frequently associated with treatment [16]. In addition, the use of such molecules might also increase the risk of activating protumor, inhibitory, or regulatory T cells (Tregs), which could reduce the efficacy of these immunotherapies [17].

TCEs that specifically activate selected T cell subsets such as $\gamma\delta$ T cells have been proposed to address these important issues [18–22]. In humans, $\gamma\delta$ T cells are distributed into four major subsets identified according to the expression of the TCR δ chain variable segment: $V\delta 1^+$, $V\delta 2^+$, $V\delta 3^+$, and $V\delta 5^+$ populations. The major peripheral blood subset in healthy human adults is highly conserved, devoid of alloreactivity, and expresses a TCR composed of a $V\delta 2$ chain that is almost exclusively associated with a TCR $V\gamma 9$ chain, whereas $V\delta 1^+$ and $V\delta 3^+$ T subsets are most frequently found in tissues [23]. A compelling set of studies has shown that $V\gamma 9V\delta 2$ T cells can directly kill tumor cells and express proinflammatory cytokines involved in the clearance of tumor cells, supporting the development of immunotherapies engaging this T lymphocyte subset [24–26].

In this study, we challenged $\alpha\beta$ T cells and unconventional $\gamma\delta$ T cells using TCEs directed against the tumor antigen CEACAM5 (CEA) in an in vitro colorectal cancer model. Our results show that $\gamma\delta$ T cells display a differential TCE-mediated antitumor response versus conventional $\alpha\beta$ T cells. Moreover, our results suggest that TCEs that can selectively target $V\gamma 9V\delta 2$ T cells could have an

enhanced therapeutic safety window by reducing cytokine release syndrome.

Materials and methods

T cell Engager molecules

VHH sequences directed against TCR $\gamma\delta$, TCR $\alpha\beta$, and CD3 were retrieved from patent applications WO2015/156673 (#5C8; #6H1), WO2016/180969 (#56G05) and WO2016/180982 (#117G03), respectively. VHH sequences directed against CEACAM5 and FMDV have been previously published [27, 28]. DNA sequences for VHHs were synthesized by GeneArt (Life Technologies) as string DNA fragments and cloned into a eukaryotic expression vector fused with human CH1 or CL domains. FreeStyle™ HEK293-F cells (Gibco, RRID:CVCL_6642) were cotransfected with two plasmids, each encoding one of the Fab chains. After 7 days, culture media were harvested and filtered before purification of the constructs on nickel-affinity columns.

Reagents

AF647-conjugated anti-CD107a (#H4A3, RRID:AB_1227506), PE-conjugated anti-PD1 (#EH12.2H7, RRID:AB_940483), AF647-conjugated anti-perforin (#dG9, RRID:AB_493255) and FITC-conjugated anti-V γ 9 (#B3, RRID:AB_1236403) monoclonal antibodies (mAbs) were purchased from BioLegend. BV510-conjugated anti-CD4 (#SK3, RRID:AB_2870492) and BV421-conjugated anti-CD8 (#RPA-T8, RRID:AB_11153676) mAbs were purchased from BD Bioscience. FITC-conjugated anti V δ 2 (#IMMU389, RRID:AB_131019) and PE-conjugated anti CD69 mAbs (#TP1.55.3, RRID:AB_2801272) were purchased from Beckman Coulter. APC-conjugated anti-V δ 1 mAb (#REA173, RRID:AB_2733451) was purchased from Miltenyi.

Cell lines

LS174T (human colon carcinoma, RRID:CVCL_1384), LS174T_shGFP (LS174T cell line stably transduced with lentiviral vector FG12.34 expressing short half-life variant green fluorescent protein), HEK293 (human embryonic kidney 293, RRID:CVCL_0045), and HEK EBNA_CEA⁺ (HEK293 cell line stably expressing Epstein–Barr virus nuclear antigen-1 and CEACAM5) cells were grown in low-glucose (1 g/L) DMEM-GlutaMax medium (Life Technology) supplemented with 10% heat-inactivated fetal calf serum (FCS) in a humidified chamber at 37°C and 5% CO₂. HEK293 (CRL-1573) and LS174T (CL-188) cells were purchased from the American Type Culture Collection. FreeStyle HEK293-F cells were cultured in Freestyle 293 expression medium (Gibco).

Isolation and amplification of human T cells

Human peripheral blood mononuclear cells (PBMCs) were isolated from the blood of healthy donors (informed consent) obtained from Etablissement Français du Sang (Nantes, France; convention # CPDL-PLER-2022 029). PBMCs were collected by Ficoll gradient centrifugation and resuspended in RPMI-1640 medium supplemented with 5% heat-inactivated FCS. T cells were enriched from PBMCs by 30 min-incubation at 37°C in a horizontal tissue-culture flask (up to 7.10^6 cells/mL) to promote the adhesion of monocytes, macrophages, and B cells. T cell-enriched supernatants were obtained by centrifugation and used directly or were frozen in heat-inactivated FCS plus 10% DMSO.

Human V γ 9V δ 2 T cells were specifically expanded from fresh PBMCs ex vivo using 5 μ M zoledronic acid (Sigma Aldrich) or 3 μ M BrHPP (bromohydrin pyrophosphate, kindly provided by Innate Pharma) in RPMI 1640 culture medium supplemented with 10% heat-inactivated FCS, 2 mM L-glutamine, 100 μ g/mL streptomycin, and 100 IU/mL recombinant human IL-2 (rhIL-2) (Proleukin, Novartis). After 4 days of culture, T lymphocytes were supplemented with rhIL-2 (300 IU/mL). After 3 weeks (resting state time), the purity of V δ 2⁺ T cells was checked using flow cytometry (85% < purity >95%). Nonspecific amplifications were performed using PHA-feeders: Phytohemagglutinin-L (Sigma-Aldrich) and 35 Gy-irradiated allogeneic feeder cells composed of human PBMC and Epstein-Barr virus-transformed B-lymphoblastoid cell lines [29]. Expanded V γ 9V δ 2 T cells were maintained in RPMI 1640 culture medium supplemented with 10% heat-inactivated FCS, 2 mM L-glutamine, 100 μ g/mL streptomycin, and 300 IU/mL rhIL-2.

Human $\alpha\beta$ T cells were expanded from fresh PBMCs by incubation with ImmunoCult human CD3/CD28 Activator (StemCell) in RPMI 1640 culture medium supplemented with 10% heat-inactivated FCS, 2 mM L-glutamine, 100 μ g/mL streptomycin, and 100 IU/mL rhIL-2. After 12 days of expansion, the purity of the amplified $\alpha\beta$ T cells was checked by flow cytometry (85% < purity >95%).

T cell activation assays

For CD107a surface mobilization assays, target cells were co-cultured for 4 h with amplified T cells (E/T ratio 1:1) in the presence of TCE (concentration range: 10 fM-1 nM) in culture medium containing 5 μ M Monensin (Sigma Aldrich) and anti-human CD107a mAb. For CD69 expression, LS174T cells were co-cultured with fresh T cell-enriched PBMCs for 24 h (E/T ratio 10:1) in the presence of TCE (concentration range: 10 fM-1 nM). The gating strategy for the different T cell subsets is represented in Fig. S1. Extracellular marker staining was performed after co-culture by incubating with the antibody mixture for 20 min at 4°C. Flow cytometry data were acquired using the Accuri C6 (BD Biosciences, RRID:SCR_019591) or Canto II cytometer (BD Biosciences, RRID:SCR_018056) and analyzed using FlowJo software (Treestar, RRID:SCR_008520).

Cytotoxicity assays

LS174T cells were incubated with ⁵¹Cr (75 μ Ci/1.10⁶ cells) for 1 h, washed, and co-cultured with ex vivo-expanded T cells (E/T ratio 10:1) for 4 h in the presence of TCE (concentration range: 10 fM-1 nM). ⁵¹Cr-release in the supernatant was measured using a MicroBeta counter (Perkin Elmer). The percentage of target cell lysis was calculated as follows: [(experimental release – spontaneous release)/(maximum release – spontaneous release)] \times 100. Spontaneous and maximum release values were determined by adding either medium or Triton X-100 to ⁵¹Cr-labeled target cells in the absence of T cells, respectively.

Imaging of immunological synapses

5.10⁵ LS174T_shGFP cells were plated in Ibidi μ -Slide 8 wells (Ibidi GmbH) coated with CellTak adhesion matrix (Corning) overnight at 37°C. TCE (1 nM) and ex vivo-expanded T cells (E/T ratio 10:1) were then added for 30 min. Cells were fixed in 4% paraformaldehyde for 10 min at room temperature (RT) and permeabilized in PBS containing 0.1% BSA and 0.1% saponin for 20 min at RT. Nonspecific binding sites were saturated with PBS containing 10% FCS and 0.1% saponin for 20 min at RT. Cells were then labeled with anti-human perforin and phalloidin for 1 h at RT in PBS containing 0.1% BSA and 0.1% saponin. Imaging was performed using a Nikon A1 confocal microscope (60X oil immersion objective, N.A 1.4) (RRID:SCR_020318). The distance between the perforin granules and the contact area between the tumor and T cells was measured using NIS-Elements analysis software (Nikon, RRID:SCR_014329).

Cytokine/granzyme B bead-based assays

Supernatants from experiments of enriched T cell activation were collected after 24 h of co-culture with LS174T cells (E/T ratio 10:1) in the presence or absence of TCE (concentration specified for each experiment). Concentrations of released IL-2, IL-10, IL-6, TGF- β 1, IFN- γ , TNF- α , and granzyme B were measured using bead-based flow cytometry (LegendPlex, BioLegend) according to the manufacturer's protocol. Data were acquired with the Accuri C6 cytometer or the Canto HTS cytometer (BD Biosciences, RRID:SCR_018055) and analyzed using the LegendPlex software (BioLegend).

Statistical analysis

Samples collected from unrelated healthy human donors have been used in this study. Data were analyzed with GraphPad Prism software v.10 and are presented as box-and-whiskers plots or as mean \pm SD or SEM. Statistical analysis data was performed by unpaired nonparametric Mann-Whitney test or by one-way ANOVA followed by Newman-Keuls, Holm-Sidák, or two-tailed

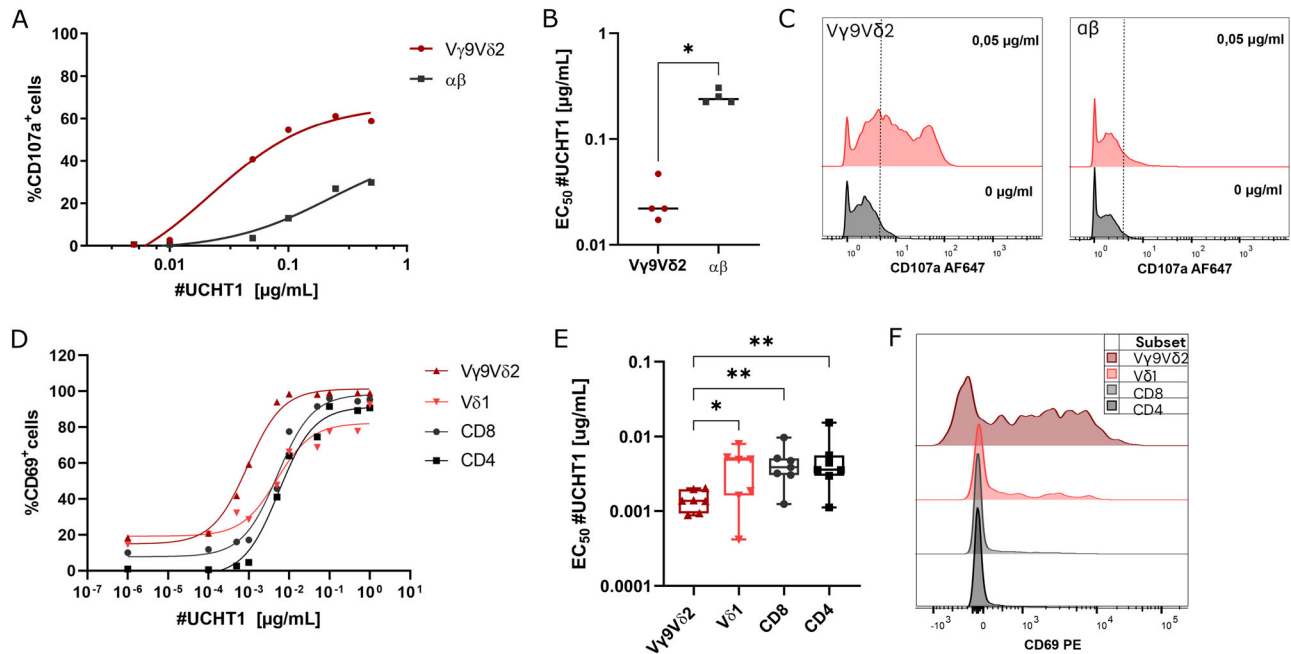


Figure 1. Anti-CD3 mAb #UCHT1 induces a stronger activation of human $\gamma\delta$ T cells, as compared with $\alpha\beta$ T cells. (A) Analysis by flow cytometry of surface expression of CD107a on ex vivo-expanded human $V\gamma 9V\delta 2$ and $\alpha\beta$ T cells after a 4 h-activation with soluble anti-CD3 mAb (#UCHT1); $n = 4$ unpaired donors. (B) Calculated activation potential (EC_{50}) from experiments shown in (A) panel; $n = 4$ unpaired donors. The unpaired Mann-Whitney test was used to assess the significance of differences between calculated EC_{50} for T cell subsets ($*P < 0.05$). (C) Representative flow cytometry histograms of CD107a surface expression on $V\gamma 9V\delta 2$ (left) and $\alpha\beta$ T cells (right) after a 4 h-activation with the 0.05 $\mu\text{g}/\text{mL}$ of #UCHT1. (D) Analysis by flow cytometry of CD69 surface expression on T cell subsets from fresh T cell-enriched PBMCs after a 24 h activation with soluble anti-CD3 mAb (#UCHT1); $n = 7$ donors. (E) Calculated activation potential (EC_{50}) from experiments shown in panel (C); $n = 7$ donors. Statistical analysis was performed using one-way ANOVA tests on log-transformed data with cell population as fixed effect and donor as a random effect, followed by Newman-Keuls tests to correct for multiplicity. (F) Representative flow cytometry histograms of CD69 surface expression on T cell subsets after a 24 h activation with 0.001 $\mu\text{g}/\text{mL}$ of #UCHT1. (A) and (D): graphs from representative donors. (B) and (E) EC_{50} values are shown as box-and-whiskers plots ($*P < 0.02$; $**P < 0.004$).

Dunnnett's tests to correct for multiplicity. P -values below 0.05 were considered statistically significant.

Results

Human $\alpha\beta$ and $\gamma\delta$ T cells react differently following CD3 engagement

Various studies have shown that human $\gamma\delta$ and $\alpha\beta$ T cells differ in their development, phenotype, and effector functions [23]. To investigate the underlying functional features, we compared the effects of a soluble anti-CD3 ϵ mAb on the activation of ex vivo-expanded human $V\gamma 9V\delta 2$ and $\alpha\beta$ T cells. As shown in Fig. 1A–C, anti-CD3 ϵ mAb (#UCHT1) induced higher levels of activation (monitored by CD107a cell surface expression) in $V\gamma 9V\delta 2$ T cells than in $\alpha\beta$ T cells, at both low and high mAb concentrations. In contrast, two other anti-CD3 ϵ mAb clones (#OKT3 and #HIT3a) showed an inverse profile as they activated preferentially $\alpha\beta$ T cells (Fig. S2). These results confirm previous observations in which the #UCHT1 clone mAb showed increased potency versus #OKT3 to trigger a CD3 ϵ -mediated activation in $V\gamma 9V\delta 2$ T cells [30]. Furthermore, #UCHT1-mediated activation of different $\gamma\delta$ and $\alpha\beta$ T cell subsets enriched from fresh peripheral

blood ($V\delta 2^+/V\delta 1^+$ $\gamma\delta$ T cells, $CD8^+/CD4^+$ $\alpha\beta$ T cells) demonstrated a stronger reactivity of $V\gamma 9V\delta 2$ T over $V\delta 1^+$ and $\alpha\beta$ T cells, as revealed by the comparative analysis of CD69 expression levels at cell surface (Fig. 1D–F). These results indicate that $V\gamma 9V\delta 2$ and $\alpha\beta$ T cell subsets react differently upon CD3 ϵ stimulation, the former unconventional T cell subset requiring significantly lower amounts of anti-CD3 ϵ mAb to reach strong activation levels.

Generation and validation of T cell engager molecules

Based on these results, TCE molecules were engineered with a VHH1 domain targeting either human CD3 or TCR ($V\delta 2$, $V\gamma 9$ or $\alpha\beta$ TCR) subunits, and a VHH2 domain targeting CEA. CEA is overexpressed in most human colorectal, pancreatic, lung, or breast carcinoma and is a validated tumor antigen for solid cancer immunotherapies [31, 32]. The CEA VHH2 was swapped with an irrelevant VHH2 binding foot-and-mouth disease virus (FMDV) to serve as a negative control. VHH1 and VHH2 were combined in a bispecific Fab-like format (bsFab), which relies on the substitution of the VH and VL domains of a conventional Fab with two independent VHH domains [33]. HA and His tags were further appended to the C-terminus of the CH1 domain to allow optimal detection and purification of TCE molecules (Fig. 2A). The apparent affinities (EC_{50}) of bsFabs were determined on CEA-expressing tumor cells LS174T and expanded $V\gamma 9V\delta 2$ or $\alpha\beta$

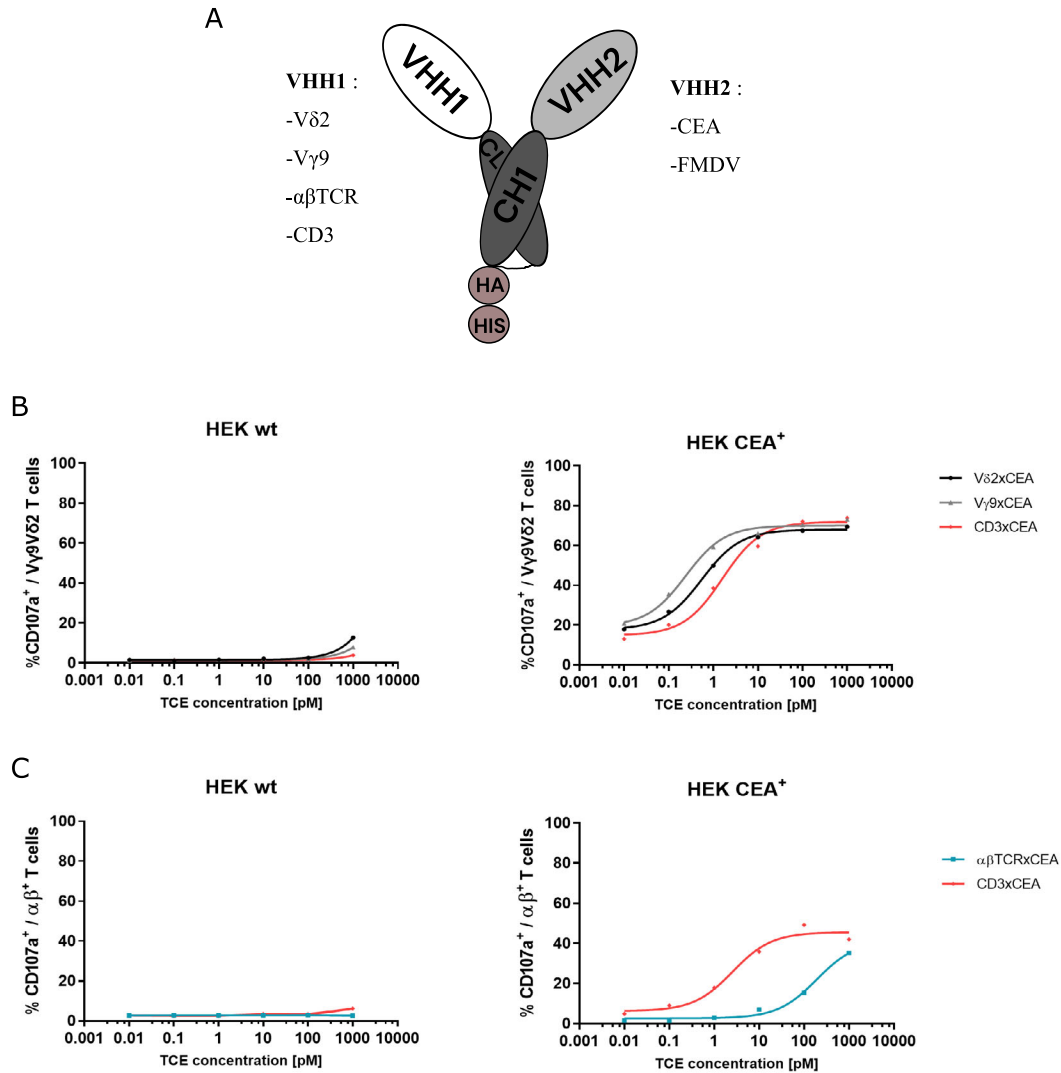


Figure 2. Design and validation of TCE molecules. (A) Schematic representation of the Fab-like TCE format and bispecific target design between VHH1 (effector T cell): Vδ2, Vγ9, αβ TCR, or CD3, and VHH2 (target cell): CEACAM5 (tumor antigen) or FMDV (negative control) fused to human CL and CH1 chains, respectively. (B) Flow cytometry analysis of CD107a expression on human ex vivo-expanded Vγ9Vδ2 T or (C) αβ T cells after a 4 h co-culture with wild-type or CEACAM5-expressing HEK293 cells (E/T ratio 1:1) in presence of xCEA bsFabs; n = 3 donors. Data from a representative donor.

Table 1. EC₅₀ calculated from binding curves of TCEs on LS174T cell line, ex vivo-expanded Vγ9Vδ2 and αβ T cells.

	Vγ9Vδ2 T		αβ T		LS174T	
	xCEA	xFMDV	xCEA	xFMDV	xCEA	xFMDV
Vδ2	1.3	0.2	>1000	>1000	1.3	>1000
Vγ9	0.6	4.6	>1000	>1000	1.8	>1000
TCRαβ	>1000	>1000	107	84.4	0.8	>1000
CD3	3.9	96.6	6.9	15.7	0.02	>1000

Note: Values are expressed in nM.

T cells (Table 1). CD3 bsFabs displayed close affinity values for both Vγ9Vδ2 and αβ T cells (3.9 nM vs 6.9 nM for CD3xCEA; 97 nM vs 16 nM for CD3xFMDV). Importantly, bsFabs with VHH1 targeting TCR subunits specifically bound to their associated T cell subsets albeit with contrasted affinity values (approximately 100 nM for αβTCR bsFabs vs nM range for Vδ2- and Vγ9-based bsFabs). Finally, all CEA bsFabs bound LS174T tumor cells with strong affinity, whereas as expected, the FMDV-based bsFabs did not bind these cells. Both the specificity and functionality of bsFabs were then assessed in a co-culture assay using HEK293 cells, either wild-type or stably expressing CEA. Expanded Vγ9Vδ2 T cells were strongly activated by Vγ9-, Vδ2-, or CD3xCEA bsFabs (Fig. 2B) when co-cultured with CEA-expressing

HEK293 cells. $\alpha\beta$ T cells were activated to a lesser extent by $\alpha\beta$ TCR- or CD3xCEA bsFabs (Fig. 2C). For all bsFabs, the activation was dose-dependent and only detected in the presence of CEA-positive cells. These results demonstrate that all bsFabs are functionally active and have the capacity to activate the desired T cell subsets in a tumor-antigen-dependent manner.

Ex vivo-expanded human V γ 9V δ 2 T cells are activated by bsFabs in the presence of CEA-expressing tumor cells

The human colon carcinoma cell line LS174T, which expresses endogenously CEA, was further used to test, and compare the specificity and potency of bsFabs in activating ex vivo-expanded V γ 9V δ 2 and $\alpha\beta$ T cells in a dose-response assay. LS174T and T cells were co-cultured (E/T ratio: 1:1) in the presence of CEA or FMDV bsFabs. T cell activation was monitored by measuring the membrane expression of CD107a. As shown in Fig. 3A, V δ 2-, V γ 9- and CD3xCEA bsFabs activated V γ 9V δ 2 T cells with sub pM potency ($EC_{50} = 0.6 \pm 0.24$ pM; 0.47 ± 0.17 pM; 0.56 ± 0.42 pM, respectively). In contrast, FMDV TCEs induced a very low level of activation, only at the highest tested doses (~ 1 nM) (Fig. S3A), confirming that bsFabs were active in a tumor antigen-dependent manner. In addition, V δ 2- and V γ 9xCEA bsFabs specifically activated V γ 9V δ 2 T cells with equivalent potency and efficacy and failed to activate $\alpha\beta$ T cells. $\alpha\beta$ T cells were exclusively activated by either $\alpha\beta$ TCR- or CD3xCEA bsFabs. However, a 50-fold higher potency was measured for CD3 bsFab over the $\alpha\beta$ TCR bsFab ($EC_{50} = 1.8 \pm 0.12$ pM vs 47.7 ± 2.7 pM) (Fig. S3B). Moreover, the plateau of $\alpha\beta$ T cell activation induced by CD3xCEA bsFab was much lower than that of V γ 9V δ 2 T cells (55 ± 0.46 % vs. 87 ± 5.6 %).

Following cell expansion, the relative CD8 and CD4 T cell frequency varied substantially between donors (Fig. S3C). We measured separately the activation of both CD8⁺ and CD4⁺ $\alpha\beta$ T cells upon treatment with $\alpha\beta$ TCR- and CD3xCEA bsFabs (Fig. 3D) and observed a dramatic difference between the maximal percentage of activated CD4⁺ $\alpha\beta$ T and CD8⁺ $\alpha\beta$ T cells in response to each bsFab (25.89 ± 3.7 vs 58.32 ± 5.1 % for $\alpha\beta$ TCR bsFab; 39.69 ± 4.2 vs 71.95 ± 3.4 % for CD3 bsFab). Of note, the CD8⁺ $\alpha\beta$ T cell subset showed a slightly lower activation efficacy (71.95 ± 3.4 % vs 87.10 ± 5.6 %) and potency (0.97 ± 0.4 % vs 0.56 ± 0.4 pM) than V γ 9V δ 2 T cells when activated with the CD3xCEA bsFab.

The T cell-directed cytotoxicity induced by bsFabs against LS174T was next measured (Fig. 3B). At E/T ratio of 10:1, V γ 9V δ 2 T cells potently killed tumor cells at sub pM concentrations of V δ 2-, V γ 9-, and CD3xCEA TCEs (left panel, $EC_{50} = 0.6 \pm 0.24$ pM vs 0.47 ± 0.17 pM vs 0.56 ± 0.42 pM, respectively) in a tumor-antigen dependent manner (FMDV bsFab effect shown in Fig. S3E, left). Similarly, $\alpha\beta$ T cells killed tumor cells in the presence of CEA bsFabs only (CEA bsFabs in Fig. 3B right and FMDV bsFab in Fig. S3E, right). A 26-fold difference in potency was measured between CD3- and $\alpha\beta$ TCRxCEA bsFabs ($EC_{50} = 0.2 \pm 0.4$

pM vs 5.2 ± 5.2 pM, respectively) and the maximal killing levels by $\alpha\beta$ T cells was much weaker as compared with V γ 9V δ 2 T cells when activated with the CD3xCEA bsFab (39.9 ± 3.7 vs 82 ± 3.8 %, respectively).

To investigate the effects of bsFabs in more detail, expanded T cells were co-cultured with GFP-transduced LS174T cells (E/T ratio 10:1), in the presence or absence of CEA bsFabs, and stained for F-actin and perforin. This allows monitoring of the translocation of perforin granules toward the contact area established between T cells and target cells as a marker of an active immunological synapse (Fig. 3C). In the absence of TCE bsFabs, the intracellular pool of perforin granules (P) was located on the opposite side of the contact zone (C). By contrast, when CEA bsFabs were added to the co-culture, perforin granules migrated rapidly (within 30 min) toward the contact zone, resulting in a significant decrease in the distance between perforin granules and the immunological synapse regardless of the bsFabs and T cell subset (Fig. 3D).

Altogether, these results show that bsFabs mediate specific interactions between T- and tumor cells in an antigen-dependent manner, resulting in their lysis via a perforin-based mechanism.

Both CD3 and TCR-specific bsFabs strongly activate human $\gamma\delta$ T cells in PBMCs

The stimulatory activity of bsFabs was investigated using fresh T cell enriched PBMCs isolated from the peripheral blood of healthy donors at an E/T ratio of 10:1. The results showed that CEA bsFabs activate T cell subsets in both a dose-dependent and VHH-specific manner when co-cultured with CEA-expressing cells (Fig. 4A and B). They also confirmed that the CD3xCEA bsFab activated CD4⁺ and CD8⁺ $\alpha\beta$ T cells more than the $\alpha\beta$ TCRxCEA bsFab, whereas the stimulatory activity of V γ 9-, V δ 2-, and CD3xCEA bsFabs on V γ 9V δ 2 T cells was comparable. Importantly, the calculated EC_{50} values of the CD3xCEA TCE for each T cell subset showed an increased potency to activate V γ 9V δ 2 T cells, as compared with other T cell subsets, including CD8⁺ $\alpha\beta$ T cells (Fig. 4C).

Co-culture supernatants were collected 24 h after treatment with the EC_{90} concentration of each TCE (Table 2), and the levels of secreted pro- or anti-inflammatory cytokines were measured (Fig. 4D). No IL-2 was detected when T cells were activated by V γ 9V δ 2-specific TCEs. While the CD3xCEA TCE and OKT3 mAb (CD3 control) induced a similarly strong release of cytokines, both V γ 9- and V δ 2xCEA bsFabs triggered significantly lower production of IFN- γ , TNF- α , and IL-6. Furthermore, these cytokines were measured at a similar level after $\alpha\beta$ TCRxCEA bsFab treatment, despite the lower E/T ratio of V γ 9V δ 2 T over $\alpha\beta$ T cells (Fig. 4E). Cytokine production per T cell upon treatment with $\alpha\beta$ TCR- and V δ 2-specific TCEs was calculated. This shows that these TCEs elicit a stronger proinflammatory response from V γ 9V δ 2 T lymphocytes compared with $\alpha\beta$ T cells, with higher production of IFN- γ , TNF- α , and IL-6 cytokines (Fig. S4A). This observation was partly confirmed when activating ex vivo-expanded V γ 9V δ 2 T and $\alpha\beta$ T cells

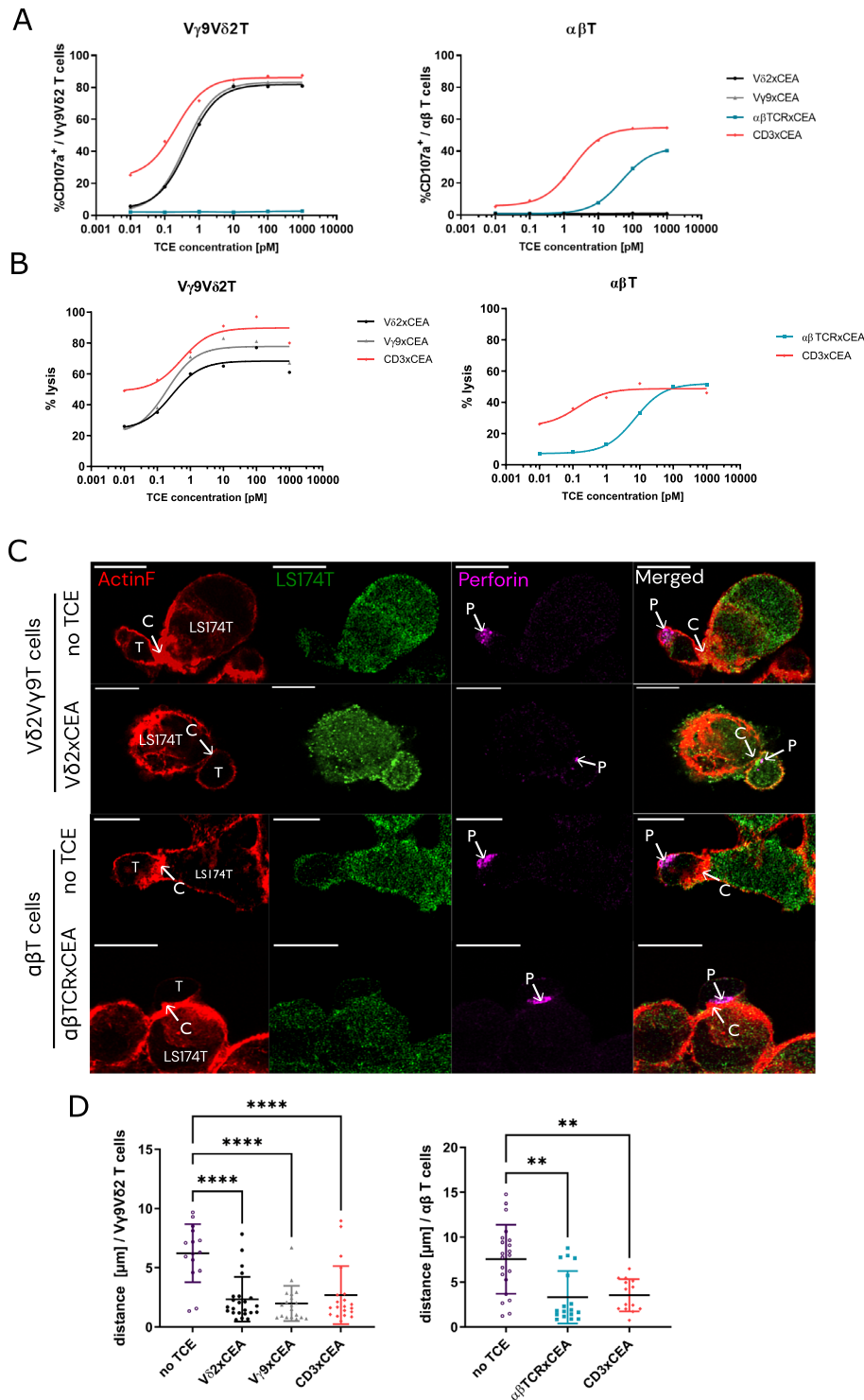


Figure 3. Comparison of bsFabs activation potency between ex vivo-expanded V γ 9V δ 2 and $\alpha\beta$ T cells. (A) Analysis by flow cytometry of CD107a expression on ex vivo-expanded human V γ 9V δ 2 (left) or $\alpha\beta$ T cells (right) after 4 h of co-culture with LS174T cells (E/T ratio 1:1), in the presence of xCEA bsFabs. *n* = 3 donors. (B) LS174T cells were loaded with ⁵¹Cr and co-cultured for 4 h with ex vivo-expanded human V γ 9V δ 2 (left) or $\alpha\beta$ T cells (right) at E/T ratio of 10:1, in the presence of xCEA bsFabs. ⁵¹Cr release was measured in culture supernatants; *n* = 4 unpaired donors. (C) Confocal microscopy images of V γ 9V δ 2 and $\alpha\beta$ T cells co-cultured with LS174T_GFP (green) for 30 min (E/T ratio 10:1) in the presence or absence of V δ 2-, or $\alpha\beta$ TCRxCEA TCEs (1 nM), before staining with phalloidin-AF568 (ActinF, red) and anti-human perforin antibody-AF647 (magenta). White arrows [C = contact, P = perforin]; scale bars = 10 μ m [60 \times magnification]. (D) Measurement of the distance between perforin granules and the contact point between V γ 9V δ 2 or $\alpha\beta$ T cells and LS174T (E/T ratio 10:1) from confocal microscopy images in the presence, or absence, of xCEA bsFabs (1 nM); *n* = 12 to 23 images per condition. Statistical analysis was performed using one-way ANOVA followed by Dunnett tests to correct for multiplicity (***P* < 0.003; *****P* < 0.0001). (A–C) Data were presented from one representative donor. (D) Data presented are individual values and their means \pm SD

at the same E:T ratio. Upon activation, ex vivo-expanded V γ 9V δ 2 T cells produced more IL-2 and TNF- α than $\alpha\beta$ T cells (Fig. S5A and C). IFN- γ production was similar for both T cell subsets, whereas IL-6 production was higher for $\alpha\beta$ T cells than V γ 9V δ 2 T cells (42 pg/mL vs 167 pg/mL upon CD3xCEA bsFab treatment respectively; Fig. S5B and D).

To assess the contribution of the perforin/granzyme killing pathway during TCE engagement, the levels of granzyme B released in the co-culture supernatant at a saturating bsFab concentration (1 nM) were measured (Fig. 4F). V γ 9-, V δ 2-, and $\alpha\beta$ TCRxCEA bsFabs induced a comparable release of granzyme B by T cell-enriched PBMCs when co-cultured with LS174T cells,

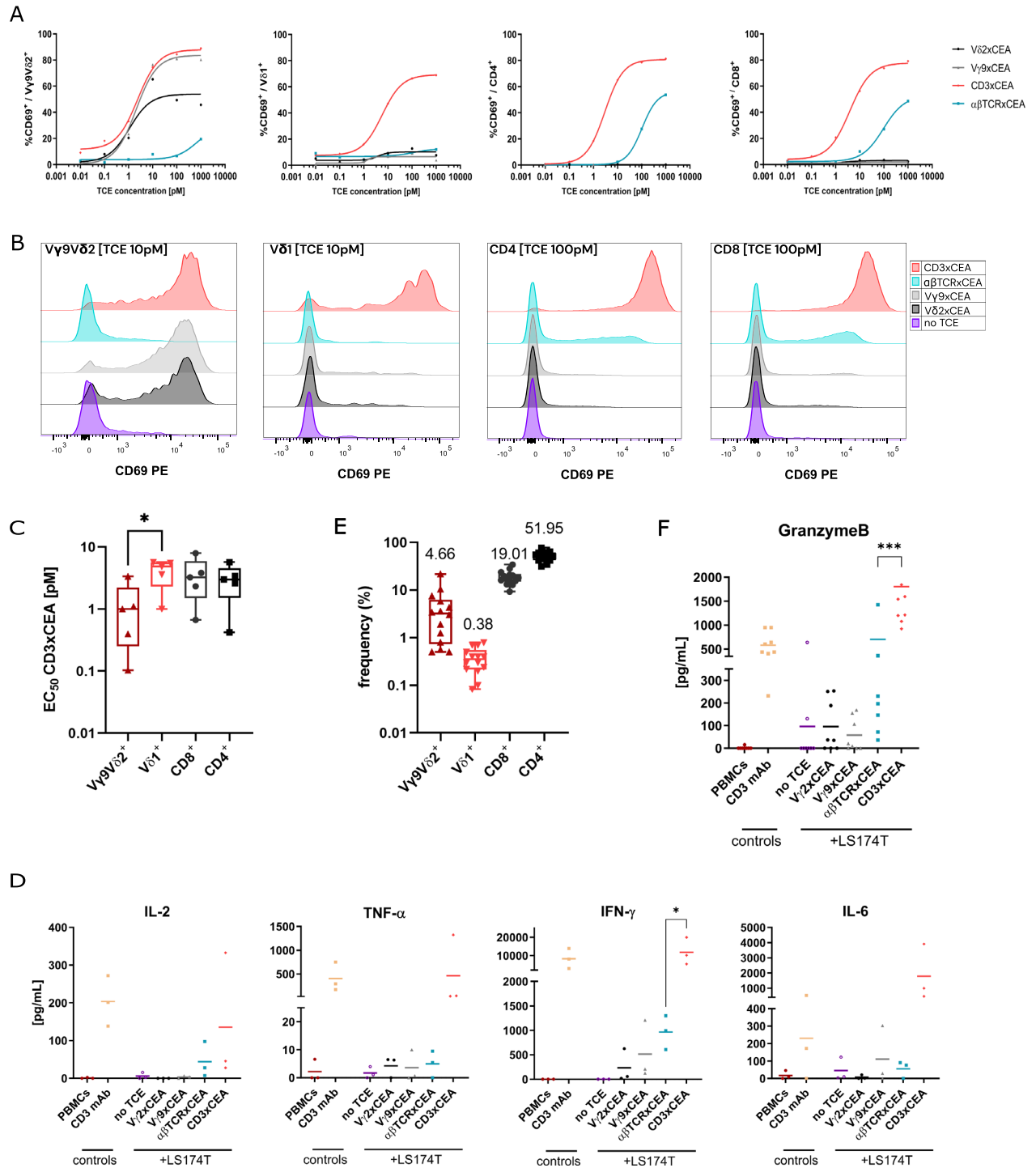


Figure 4. CEA bsFabs specifically activate human peripheral T cells. (A) Analysis by flow cytometry of CD69 surface expression on T enriched PBMCs after a 24 h-co-culture with LS174T target cells (E/T ratio 10:1), in the presence of xCEA bsFabs; $n = 5$ donors. (B) Representative flow cytometry histograms of CD69 surface expression on T cell subsets after a 24 h-co-culture with LS174T target cells (E/T ratio 10:1), in the presence of xCEA bsFabs. Data were presented from one representative donor. (C) Calculated activation potential (EC_{50}) from experiments with CD3 bsFab (calculated from Fig. 4A); $n = 5$ donors. Statistical analysis was performed using one-way ANOVA followed by Holm–Sidak test to correct for multiplicity ($*P < 0.05$). (D) IFN- γ , IL-2, TNF- α , and IL-6 concentration measured in the 24 h supernatant of fresh T cell-enriched PBMCs co-cultured with LS174T cells (E/T ratio 10:1), in presence or absence of xCEA bsFabs at their EC_{90} (calculated from Fig. 4A); $n = 3$ donors. (E) Frequencies of $V\delta 2^+$, $V\delta 1^+$, $CD4^+$, and $CD8^+$ T cell subsets in fresh T cell-enriched PBMCs measured by flow cytometry; $n = 14$ donors. (F) Granzyme B release in the 24 h supernatant of fresh T cell-enriched PBMCs co-cultured with LS174T cells (E/T ratio 10:1) in the presence or absence of xCEA bsFabs (1 nM); $n = 8$ donors. (C, E) Data shown as box-and-whiskers plots. (D, F) Data presented as individual values and their mean — statistical analysis performed by one-way ANOVA followed by two-tailed Dunnett’s tests for no TCE, $V\delta 2$ xCEA, $V\delta 1$ xCEA, and $CD3$ xCEA vs $\alpha\beta$ TCRxCEA ($*P < 0.05$; $***P < 0.0005$) — nonsignificant differences are not displayed in the figure.

Table 2. EC₉₀ calculated from CD69 expression curves after activation of Tcell-enriched PBMCs by TCEs and SD; n = 5 donors.

	Subset	EC ₉₀ (pM)	SD
Vδ2xCEA	Vγ9Vδ2	6.462	3.283
Vγ9xCEA	Vγ9Vδ2	15.03	5.791
αβTCRxCEA	αβCD8	1091	341.1
CD3xCEA	αβCD8	26.85	11.91

Note: Values are expressed in pM.

which reflects a higher secretion by Vγ9Vδ2 T than αβ T cells as shown by normalizing to the cell number (2.3 ± 2.8 fg/cell treated with Vδ2 bsFab vs 0.99 ± 1.3 fg/cell treated with αβTCR bsFab; Fig. S4B).

Altogether, these results indicate that Vγ9-, Vδ2- and CD3xCEA bsFabs efficiently activate the innate-like peripheral human Vγ9Vδ2 T cell subset and that Vγ9Vδ2 T cell-specific activation triggers potent antitumor functions, such as perforin/granzyme B-dependent cytolysis with decreased release of proinflammatory cytokines.

Vγ9Vδ2-specific bsFabs fail to induce the expression or release of inhibitory molecules

Finally, the induction of immunosuppressive or protumoral features by bsFabs was investigated. First, the level of PD-1 surface expression was measured in fresh T cell subsets after 24 and 48 h of co-culture with LS174T cells (E/T ratio 10:1) in the presence of a saturating dose of bsFabs (1 nM). Interestingly, γδ and αβ T cells exhibited different responses to bsFab-induced stimulation. Upregulation of PD-1 expression on Vγ9Vδ2 T cells was observed only with CD3xCEA bsFab at 48 h, but not with Vγ9-, or Vδ2xCEA bsFabs. In contrast, αβ T cells displayed peak PD-1 expression at 24 h after stimulation with both CD3- and αβTCRxCEA (Fig. 5A and B).

The supernatants from the co-cultures of fresh T cell-enriched PBMCs and LS174T cells were collected at 24 h and the production of IL-10 and TGF-β1 were measured. At the EC₉₀ concentrations of TCEs (Table 2), there was no detectable IL-10 production in the Vγ9- and Vδ2xCEA bsFabs supernatants (Fig. 5C), while IL-10 was observed when T enriched PBMCs were treated with CD3- and αβTCRxCEA bsFabs. Similarly, after 16 h of incubation with a saturating dose of TCEs, no IL-10 was detected in the supernatants of ex vivo-expanded Vγ9Vδ2 T cells (Fig. S5E). Interestingly, the specific activation of αβT cells by the αβTCRxCEA bsFab showed a distinct pattern with significant production of TGF-β1 while the activation by the two Vγ9Vδ2 TCR-specific bsFabs did not induce the production of TGF-β1 (Fig. 5D). CD3xCEA bsFab induced similar levels of TGF-β1 as Vγ9- and Vδ2-CEA bsFabs. Collectively, these results suggest that activation of fresh T cell-enriched PBMCs by Vγ9Vδ2 TCR-specific bsFabs, in contrast to CD3 and αβTCR bsFabs, does not induce surface expression or release of regulatory molecules known for their negative effects on immune responses within the tumor environment.

Discussion

The ever-increasing number of TCEs progressing to clinical trials and the recent approvals of multiple CD20 and BCMA TCEs for the treatment of hematological malignancies highlight the considerable therapeutic potential of tumor-specific T cell agonism [34]. These immunotherapies suffer however from severe limitations such as side effects or nonoptimal efficacy leading the patient to discontinue therapy. CRS, infections, and neurotoxicity are common side effects whose occurrence and severity depend on TCE and indications [35]. Solid cancer treatment by TCEs increases the challenge due to the potential lower accessibility to the tumor target and a higher risk of off-target toxicity [36, 37].

This mechanistic study aimed at investigating alternative TCE strategies to reduce side effects while keeping a potent anti-tumor response in solid cancers by specifically targeting human γδ T cell subsets which can account for up to 50% of tissue-resident T cells and for an important proportion of tumor-infiltrated T cells (TILs) [38, 39]. We performed an in vitro comparative functional study of TCEs targeting either all T cells, conventional αβ T cells, or unconventional Vγ9Vδ2 T cells. Whereas TCEs that target CD3 and Vγ9 TCR chains have been previously described, our study is, to our knowledge, the first to propose a full in vitro and ex vivo comparison with a single TCE format [40]. The reactivities of these T cell subsets to CD3 TCEs or TCEs specific to each T cell population were investigated; more precisely, their activation level, cytokine production, tumor cell-killing capacity, and plasticity to display an immunomodulatory phenotype were compared.

The use of ex vivo-expanded T cells, with similar purity ranges, allowed us to study and compare the specific potential of CD3-based TCEs on both αβ T and Vγ9Vδ2 T cells with comparable E:T ratios. Our results showed that the activation of Vγ9Vδ2 T cells by the CD3 bsFab outperformed that of αβ T cells based on a higher surface mobilization of the degranulation marker CD107a and enhanced maximal tumor cell killing. Furthermore, treatment of T cell enriched PBMCs with the CD3 TCE resulted in the activation of all T cell subsets and confirmed the higher sensitivity of Vγ9Vδ2 T cells to CD3 stimulation when compared with αβ T cells. Importantly, the Vγ9Vδ2-specific TCEs were as potent and efficient as the CD3 bsFab to elicit both Vγ9Vδ2 T cell activation and cytolytic activity, in an antigen-dependent manner. In contrast, the αβ T cell response to the αβTCR-specific TCE was found to be much less potent than to the CD3 TCE. This could be related to the different affinities of these two TCEs for αβ T cells (≈7 vs 100nM for CD3xCEA vs αβ TCRxCEA bsFabs) or to their different epitopes on the full αβ TCR.

The in vitro potency of CD3-based bispecific TCEs is influenced by several key factors [41]. The spatial arrangement of their binding domains is essential and modifying the relative positioning of the antigen-binding domain and the CD3-binding domain, either through changes in the TCE format or variations of the binding domains themselves, results in distinct binding geometries to the target cells and dictates the size of the synapse as well as the extent of the CD3 conformational change [42]. This, in

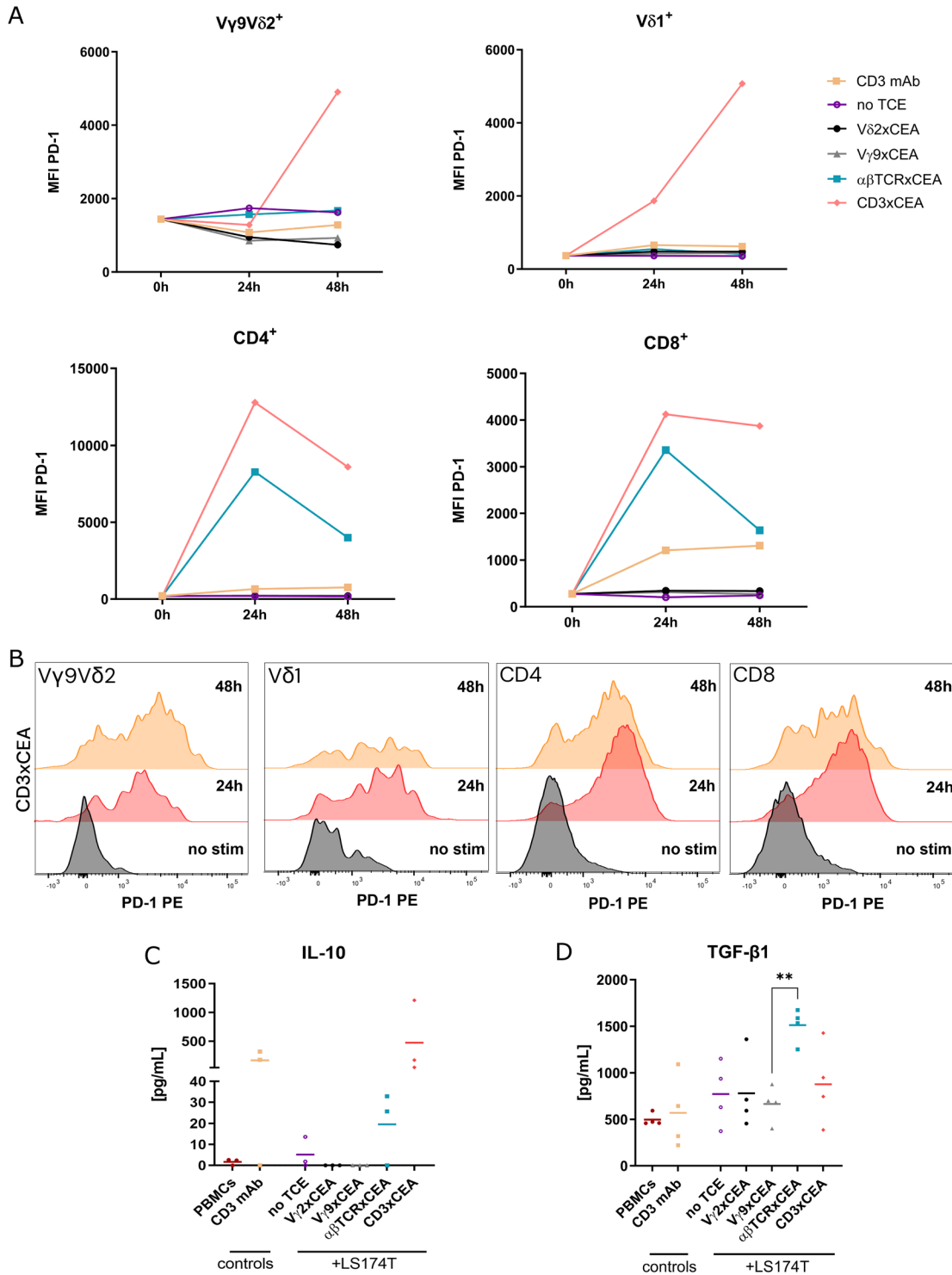


Figure 5. The activation of fresh human peripheral $\gamma\delta$ T cells by bsFabs does not induce the expression of exhaustion markers or regulatory molecules. (A) Analysis by flow cytometry of surface PD-1 expression (median of fluorescence) on T cell-enriched PBMCs after 0, 24, or 48 h of co-culture with LS174T cells (E/T ratio 10:1) in the presence or absence of xCEA bsFabs (1nM), gated on V δ 2⁺, V δ 1⁺, CD4⁺ or CD8⁺ cells; n = 2 donors. For each of the four subsets, the data presented corresponds to the MFI (median) of PD-1 expression. (B) Representative flow cytometry histograms of PD-1 surface expression on T cell subsets after 0, 24, or 48 h of co-culture with LS174T target cells (E/T ratio 10:1), in the presence of CD3xCEA bsFab (1 nM). (C) IL-10 concentration measured in the 24 h-supernatants of fresh T cell-enriched PBMCs co-cultured with LS174T cells (E/T ratio 10:1), in the presence, or absence, of xCEA bsFabs at their EC₅₀ (calculated from Fig. 4A); n = 3 donors. (D) Measurement of total TGF- β 1 in 24 h-supernatants of fresh T cell-enriched PBMCs co-cultured with LS174T in the presence or absence of xCEA bsFabs (1 nM); n = 4 donors. (C, D) Data were presented as individual values and their mean. Statistical analysis was performed using one-way ANOVA followed by two-tailed Dunnett's tests for $\alpha\beta$ TCRxCEA vs no TCE, V δ 2xCEA, V γ 9xCEA, and CD3xCEA (**P < 0.01) — nonsignificant differences are not displayed in the figure.

turn, influences T cell activation efficacy, and subsequently cell killing potency and cytokine release [41]. In our study, the format and the binding domain to the tumor antigen are fixed. Given the diversity of variable domains in the TCR chains of $\alpha\beta$ T cells, the $\alpha\beta$ TCR VHH is likely to bind the TCR constant domain. Unfortunately, the absence of structural information on the VHHs (V δ 2, V γ 9, and $\alpha\beta$ TCR) limits our ability to precisely understand how the corresponding bsFabs arrange on the TCR surface and influence the overall synapse topology. Furthermore, the affinities of the TCEs for both CD3 and the tumor antigen are known to contribute to the tightness of the interaction and play a critical role in *in vitro* T cell activation and killing potency. In this study, the affinities of the TCR-specific bsFabs for the tumor antigen are very similar and therefore cannot account for the observed potency difference. In contrast, there is a 2-log difference in affinity for their cognate T cells in favor of the two $\gamma\delta$ T-specific bsFabs. Lowering the affinity of T cell engagers for the target CD3 is known to limit *in vitro* T cell activation [43]. If this holds true when targeting the TCR chains instead of the CD3 subunits, it could be the main factor contributing to the observed potency difference. An interesting avenue for exploration involves comparing bsFabs built with VHH affinity variants for either the $\alpha\beta$ or V γ 9V δ 2 TCR.

The cytolytic activity of all expanded T cell subsets induced by all bsFabs involved the perforin/granzyme pathway as previously reported for other CD3-based TCEs on CD4⁺ and CD8⁺ T cells [4]. We showed that within 30 min after the addition of any bsFabs, both $\alpha\beta$ T and V γ 9V δ 2 T cells have their perforin granules relocated to the immune synapse. The difference in killing activity levels that we measured for the two T cell subsets treated with the CD3 bsFab could be explained by various parameters such as the effector differentiation state and the number of responding T cells, or intrinsic granzyme B loading [44]. Circulating V γ 9V δ 2 T cells have an innate-like and memory phenotype [45]. Consequently, they require a lower threshold for early antigenic activation and can bypass the need for CD28 costimulation to acquire a potent cytotoxic function as confirmed by our experiments using a monoclonal anti-CD3 mAb. Interestingly, several studies have shown that the lack of a costimulatory signal 2 leads to a nonoptimal CD4⁺/CD8⁺ T cell stimulation by CD3 TCEs and that an additional tumor-specific CD28 stimulation is a promising strategy to improve antitumor activity of CD3 bispecific T cell engagers [46].

A major adverse effect triggered by TCE-based therapies is the massive production of inflammatory cytokines associated with an overactivation of the immune system, also known as CRS. High-grade CRS is generally manageable but requires patient hospitalization and can be life-threatening for the patient [47–49]. This has led to recent engineering strategies aimed at decreasing CD3 binding domain affinities or designing conditionally active TCEs [50–52]. An alternative strategy to improve the safety profile of bispecific TCEs while keeping high antitumor activity is to selectively recruit highly cytotoxic T cell subsets such as $\gamma\delta$ T cells rather than indiscriminately recruit all T cells (reviewed in [53]). We compared the effects of specific stimulation of V γ 9V δ 2 T cells by V γ 9- or V δ 2-based TCE and CD3-based TCE in T cell-enriched PBMCs. While both triggered a similar level of V γ 9V δ 2 T cell acti-

vation, specific stimulation resulted in lower levels of secreted immune effectors such as granzyme B, IFN- γ , and TNF- α , at levels correlated with the low V γ 9V δ 2: tumor cell ratio. Similarly, the secretion of IL-6, one of the most aversive cytokines in cancer immunotherapies [54], was dramatically decreased when only V γ 9V δ 2 T cells were engaged. In addition, V γ 9- or V δ 2xCEA bsFab treatment blocked the induction of immunomodulatory cytokines (e.g. regulating Treg activation) such as IL-2, IL-10, or TGF- β 1 while the CD3- and $\alpha\beta$ TCRxCEA bsFabs induced at least 2 of these 3 cytokines. Finally, the induction of PD-1 expression on the T cell surface following activation by bsFabs was found markedly different between the different T cell subsets. $\alpha\beta$ T cells rapidly upregulated PD-1 when treated with either CD3 or $\alpha\beta$ TCR bsFabs while the $\gamma\delta$ T cell response to the CD3xCEA bsFab was delayed. More strikingly, PD-1 expression was not induced on V γ 9V δ 2 T cells activated by V γ 9- or V δ 2xCEA bsFabs. This result is particularly encouraging as it has been recently reported that continuous stimulation with TCE can induce CD4⁺/CD8⁺ T cell exhaustion and ultimately lead to resistance to therapy [55].

Altogether, our results indicate that the specific activation of V γ 9V δ 2 T cells by TCEs not only induces a strong cytotoxic activity, but also (1) triggers low production of IFN- γ , TNF- α , and IL-6, which should reduce the risk of CRS as compared with large-spectrum TCEs which engage CD3 and subsequently all T cells without discrimination, (2) is characterized by no to the minimal release of modulatory cytokines such as IL-2, IL-10, or TGF- β , and (3) does not induce the expression of exhaustion markers such as PD-1, suggestive of a durable effective cytotoxic phenotype. This study therefore fully supports the development of novel $\gamma\delta$ T-bispecific cell engagers, the most advanced of which are currently being evaluated in clinical trials [53]. To progress successfully, the next steps involve comprehensive pre-clinical assessments of efficacy and safety. Given the absence of murine counterparts for human V γ 9V δ 2 T cells and the lack of animal models that fully recapitulate the intricate interplay of human cancers and immune networks, the antitumor activity and the safety of V γ 9V δ 2-targeting TCEs should be separately evaluated using distinct animal models. Immunodeficient mice carrying human tumor xenografts and injected with a partially humanized immune system through the introduction of human V γ 9V δ 2 T or PBMCs have been used to assess the antitumor efficacy of $\gamma\delta$ T specific TCEs [22, 56]. In contrast, nonhuman primates, which naturally harbor V γ 9V δ 2 T cells, can serve as a valuable model for assessing the safety profile of V γ 9V δ 2-targeting TCEs. King et al. [22] report these strategies for the characterization of a V δ 2xEGFR TCE demonstrating both its efficacy and safety. Of note, advances in hematopoietic stem cell-engrafted immunodeficient mice hold the potential to evaluate both criteria in a single preclinical model in the near future.

Human $\gamma\delta$ T cell subsets can account for an important proportion of TILs. While TILs are pivotal for effective antitumor immunity, the persistence of an immunosuppressive microenvironment that maintains TILs in an anergic or exhausted state is a major cause of tumor control escape. With this in mind, it would be interesting to generate TCEs specifically targeting other

human $\gamma\delta$ T cell subsets, such as $V\delta 1^+$ or $V\delta 3^+$ T cells. These subsets have been evidenced for their contribution to antitumor responses, especially in solid tumors [39]. Exploring the response of TILs to TCEs tailored for different $\gamma\delta$ T cell subsets could provide valuable insights. Unfortunately, the lack of VHHs targeting specifically the $V\delta 1$ or $V\delta 3$ TCR chains makes such comparative studies challenging. Finally, it would be interesting to investigate whether $\gamma\delta$ T-specific TCEs would be potent enough to overcome immunosuppression in the tumor microenvironment, and if their combination with allogeneic $V\gamma 9V\delta 2$ T cell transfer from healthy donors might help enhance the efficacy of TCEs without additional toxicity [57].

Acknowledgements: The authors thank the Cell and Tissue Imaging Center of the University of Nantes (MicroPICell) for imaging and the Cytocell Cytometry Center of Nantes for technical assistance. We thank the Automated mAb Production and Protein Science & Technology teams of the Sanofi Large Molecule Research platform (Vitry, France) for the purification of the TCEs, Laurent Vidard (Sanofi) for providing *ex-vivo* expanded $V\gamma 9V\delta 2$ T cells, and Oliver Hijano Cubelos (Sanofi) for the statistical analysis. The authors also thank Margareta Wilhelm for critical reading of the manuscript.

This work was financially supported by SANOFI (Collaboration agreement SANOFI/Université de Nantes). LB and MC were supported by a CIFRE fellowship (N°2016/0639 and N°2021/1444, respectively) funded in part by the National Association for Research and Technology (ANRT) on behalf of the French Ministry of Education and Research, and in part by SANOFI.

Conflict of interest: Lola Boutin, Clément Barjon, Morgane Chauvet, Eric Senechal, Dorothée Bourges, and Emmanuelle Vigne are Sanofi employees and may hold shares and/or stock options in the company. The remaining authors declare no financial or commercial conflict of interest.

Author contributions: Conception and design of the project: Emmanuel Scotet and Emmanuelle Vigne. Analysis and interpretation of the data: Lola Boutin, Emmanuel Scotet, and Emmanuelle Vigne. Generation and acquisition of data: Lola Boutin with inputs of Eric Senechal, Clément Barjon, Laura Lafrance, Morgane Chauvet, and Dorothée Bourges. Study methodology: Lola Boutin, Eric Senechal, and Emmanuelle Vigne. Statistical analysis: Lola Boutin. Writing, reviewing, and editing were performed by Lola Boutin, Emmanuel Scotet, and Emmanuelle Vigne, with input from Dorothée Bourges and Clément Barjon.

Data availability statement: The data that support the findings of this study are available from the corresponding authors upon reasonable request.

References

- 1 Staerz, U. D., Yewdell, J. W. and Bevan, M. J. Hybrid antibody-mediated lysis of virus-infected cells. *Eur. J. Immunol.* 1987. 17: 571–574.
- 2 Staerz, U. D., Kanagawa, O. and Bevan, M. J. Hybrid antibodies can target sites for attack by T cells. *Nature.* 1985; 314: 628–631.
- 3 Dreier, T., Lorenczewski, G., Brandl, C., Hoffmann, P., Syring, U., Hanakam, F., Kufer, P., et al., Extremely potent, rapid and costimulation-independent cytotoxic T-cell response against lymphoma cells catalyzed by a single-chain bispecific antibody. *Int. J. Cancer.* 2002. 100, 690–697 .
- 4 Haas, C., Krinner, E., Brischwein, K., Hoffmann, P., Lutterbüse, R., Schlereth, B., Kufer, P. et al. Mode of cytotoxic action of T cell-engaging BiTE antibody MT110. *Immunobiology.* 2009. 214: 441–453.
- 5 Brinkmann, U. and Kontermann, R. E. The making of bispecific antibodies. *MAbs.* 2017. 9: 182–212.
- 6 Hamers-Casterman, C., Atarhouch, T., Muyldermans, S., Robinson, G., Hamers, C., Songa, E. B., Bendahman, N., et al. Naturally occurring antibodies devoid of light chains. *Nature* 1993. 363: 446–448.
- 7 Löffler, A., Kufer, P., Lutterbüse, R., Zettl, F., Daniel, P. T., Schwenkenbecher, J. M., Riethmüller, G., et al., A recombinant bispecific single-chain antibody, CD19 x CD3, induces rapid and high lymphoma-directed cytotoxicity by unstimulated T lymphocytes. *Blood.* 2000. 95: 2098–2103.
- 8 Bannas, P., Hambach, J. and Koch-Nolte, F., Nanobodies and nanobody-based human heavy chain antibodies as antitumor therapeutics. *Front. Immunol.* 2017. 8.
- 9 Takeuchi, T., Kawanishi, M., Nakanishi, M., Yamasaki, H. and Tanaka, Y., Phase II/III results of a trial of anti-tumor necrosis factor multivalent NANOBODY compound ozoralizumab in patients with rheumatoid arthritis. *Arthritis Rheumatol.* 2022. 74: 1776–1785.
- 10 Topp, M. S., Gökbuget, N., Zugmaier, G., Stein, A. S., Dombret, H., Chen, Y., Ribera, J. M., et al. Long-term survival of patients with relapsed/refractory acute lymphoblastic leukemia treated with blinatumomab. *Cancer* 2021. 127: 554–559.
- 11 Budde, L. E., et al., Safety and efficacy of mosunetuzumab, a bispecific antibody, in patients with relapsed or refractory follicular lymphoma: a single-arm, multicentre, phase 2 study. *Lancet Oncol* 2022. 23: 1055–1065.
- 12 Tran, B., Horvath, L., Dorff, T., Rettig, M., Lolkema, M. P., Machiels, J. P., Rottey, S., et al., 6090 Results from a phase I study of AMG 160, a half-life extended (HLE), PSMA-targeted, bispecific T-cell engager (BiTE®) immune therapy for metastatic castration-resistant prostate cancer (mCRPC). *Ann. Oncol.* 2020. 31: S507.
- 13 Junttila, T. T., Li, Ji, Johnston, J., Hristopoulos, M., Clark, R., Ellerman, D., Wang, Bu-Er, et al., Antitumor efficacy of a bispecific antibody that targets HER2 and activates T cells. *Cancer Res.* 2014. 74: 5561–5571.
- 14 Belmontes, B., Sawant, D V., Zhong, W., Tan, H., Kaul, A., Aeffner, F., O'brien, S A., et al., Immunotherapy combinations overcome resistance to bispecific T cell engager treatment in T cell-cold solid tumors. *Sci. Transl. Med* 2021. 13: eabd1524.
- 15 Ma, H., Wang, H., Sové, R. J., Wang, J., Giragossian, C. and Popel, A. S.. Combination therapy with T cell engager and PD-L1 blockade enhances the antitumor potency of T cells as predicted by a QSP model. *J. Immunother. Cancer* 2020. 8: e001141.
- 16 von Stackelberg, A., et al., Phase I/Phase II Study of Blinatumomab in Pediatric Patients With Relapsed/Refractory Acute Lymphoblastic Leukemia. *J Clin Orthod* 2016. 34: 4381–4389.
- 17 Duell, J., Dittrich, M., Bedke, T., Mueller, T., Eisele, F., Rosenwald, A., Rasche, L., et al., Frequency of regulatory T cells determines the out-

- come of the T-cell-engaging antibody blinatumomab in patients with B-precursor ALL. *Leukemia* 2017. 31: 2181–2190.
- 18 Oberg, H. H., Kellner, C., Gonnermann, D., Peipp, M., Peters, C., Sebens, S., Kabelitz, D., et al., $\gamma\delta$ T cell activation by bispecific antibodies. *Cell Immunol.* 2015. 296: 41–49.
 - 19 De Weerdt, I., Lameris, R., Ruben, J. M., De Boer, R., Kloosterman, J., King, L. A., Levin, M. D., et al., A Bispecific Single-Domain Antibody Boosts Autologous $V\gamma 9V\delta 2$ -T Cell Responses Toward CD1d in Chronic Lymphocytic Leukemia. *Clin. Cancer Res.* 2021. 27, 1744–1755.
 - 20 Ganesan, R., Chennupati, V., Ramachandran, B., Hansen, M. R., Singh, S. and Grewal, I. S.. Selective recruitment of $\gamma\delta$ T cells by a bispecific antibody for the treatment of acute myeloid leukemia. *Leukemia* 2021. 35: 2274–2284.
 - 21 Lai, A. Y., Patel, A., Brewer, F., Evans, K., Johannes, K., González, L. E., Yoo, K. J., et al., Cutting edge: bispecific $\gamma\delta$ T cell engager containing heterodimeric BTN2A1 and BTN3A1 promotes targeted activation of $V\gamma 9V\delta 2$ T cells in the presence of costimulation by CD28 or NKG2D. *J. Immunol.* 2022. 209: 1475–1480.
 - 22 King, L. A., Toffoli, E. C., Veth, M., Iglesias-Guimaraes, V., Slot, M. C., Amsen, D., Van De Ven, R., et al., A bispecific $\gamma\delta$ T-cell engager targeting EGFR activates a potent $V\gamma 9V\delta 2$ T cell-mediated immune response against EGFR-expressing tumors. *Cancer Immunol Res* 2023. 11, 1237–1252.
 - 23 Hayday, A. C.. [gamma][delta] cells: a right time and a right place for a conserved third way of protection. *Annu Rev Immunol* 2000. 18: 975–1026.
 - 24 Bouet-Toussaint, F., Cabillic, F., Toutirais, O., Le Gallo, M., Thomas De La Pintièrre, C., Daniel, P., Genetet, N., et al. $V\gamma 9V\delta 2$ T cell-mediated recognition of human solid tumors. Potential for immunotherapy of hepatocellular and colorectal carcinomas. *Cancer Immunol Immunother* 2008. 57: 531–539.
 - 25 Jarry, U., Chauvin, C., Joalland, N., Léger, A., Minault, S., Robard, M., Bonneville, M., et al. Stereotaxic administrations of allogeneic human $V\gamma 9V\delta 2$ T cells efficiently control the development of human glioblastoma brain tumors. *Oncoimmunology* 2016. 5: e1168554.
 - 26 De Gassart, A., Le, K. S., Brune, P., Agaugué, S., Sims, J., Goubard, A., Castellano, R., et al. Development of ICT01, a first-in-class, anti-BTN3A antibody for activating $V\gamma 9V\delta 2$ T cell-mediated antitumor immune response. *Sci Transl Med* 2021. 13: eabj0835.
 - 27 Behar, G., Chames, P., Teulon, I., Cornillon, A., Alshoukr, F., Roquet, F., Pugnieri, M., et al., Llama single-domain antibodies directed against nonconventional epitopes of tumor-associated carcinoembryonic antigen absent from nonspecific cross-reacting antigen. *FEBS J.* 2009. 276: 3881–3893.
 - 28 Harmsen, M. M., Van Solt, C. B., Fijten, H. P. D., Van Keulen, L., Rosalia, R. A., Weerdmeester, K., Cornelissen, A. H. M., et al., Passive immunization of guinea pigs with llama single-domain antibody fragments against foot-and-mouth disease. *Vet. Microbiol.* 2007. 120: 193–206.
 - 29 Issekutz, T., Chu, E. and Geha, R. S., Antigen presentation by human B cells: T cell proliferation induced by Epstein Barr virus B lymphoblastoid cells. *J Immunol* 1982. 129: 1446–1450.
 - 30 Dopfer, E. P., Hartl, F. A., Oberg, H. H., Siegers, G. M., Yousefi, O. S, Kock, S., Fiala, G. J., et al., The CD3 conformational change in the $\gamma\delta$ T cell receptor is not triggered by antigens but can be enforced to enhance tumor killing. *Cell Rep.* 2014. 7: 1704–1715.
 - 31 Zheng, C., Feng, J., Lu, Di, Wang, P., Xing, S., Coll, J. L., Yang, D., et al., A novel anti-CEACAM5 monoclonal antibody, CC4, suppresses colorectal tumor growth and enhances NK cells-mediated tumor immunity. *PLoS One* 2011. 6, e21146.
 - 32 Dotan, E., et al., Phase I/II trial of labetuzumab Govitecan (anti-CEACAM5/SN-38 antibody-drug conjugate) in patients with refractory or relapsing metastatic colorectal cancer. *J Clin Orthod* 2017. 35: 3338–3346.
 - 33 Rozan, C., Cornillon, A., Pétiard, C., Chartier, M., Behar, G., Boix, C., Kerfelec, B., et al., Single-domain antibody-based and linker-free bispecific antibodies targeting Fc γ RIII induce potent antitumor activity without recruiting regulatory T cells. *Mol. Cancer Ther.* 2013. 12: 1481–1491.
 - 34 Tapia-Galisteo, A., Álvarez-Vallina, L. and Sanz, L., Bi- and trispecific immune cell engagers for immunotherapy of hematological malignancies. *J. Hematol. Oncol.* 2023. 16: 83.
 - 35 Swan, D., Murphy, P., Glavey, S. and Quinn, J., Bispecific antibodies in multiple myeloma: opportunities to enhance efficacy and improve safety. *Cancers* 2023. 15: 1819.
 - 36 Baeuerle, P. A. and Wesche, H., T-cell-engaging antibodies for the treatment of solid tumors: challenges and opportunities. *Curr. Opin. Oncol.* 2022. 34: 552.
 - 37 Park, D. H., Liaw, K., Bhojnagarwala, P., Zhu, X., Choi, J., Ali, A. R., Bordoloi, D., et al. Multivalent in vivo delivery of DNA-encoded bispecific T cell engagers effectively controls heterogeneous GBM tumors and mitigates immune escape. *Mol Ther Oncolytics* 2023. 28: 249–263.
 - 38 Tosolini, M., Pont, F., Poupot, M., Vergez, F., Nicolau-Travers, M. L., Vermijlen, D., Sarry, J. E., et al., Assessment of tumor-infiltrating TCRV $\gamma 9V\delta 2$ $\gamma\delta$ lymphocyte abundance by deconvolution of human cancers microarrays. *Oncoimmunology* 2017. 6: e1284723.
 - 39 Wu, Y., Biswas, D., Usaite, I., Angelova, M., Boeing, S., Karasaki, T., Veeriah, S., et al. A local human V $\delta 1$ T cell population is associated with survival in nonsmall-cell lung cancer. *Nat Cancer* 2022 3: 696–709.
 - 40 Oberg, H. H., Janitschke, L., Sulaj, V., Weimer, J., Gonnermann, D., Hedemann, N., Arnold, N., et al., Bispecific antibodies enhance tumor-infiltrating T cell cytotoxicity against autologous HER-2-expressing high-grade ovarian tumors. *J Leukoc Biol* 2020. 107: 1081–1095.
 - 41 Chen, R. P., Shinoda, K., Rampuria, P., Jin, F., Bartholomew, T., Zhao, C., Yang, F., et al. Bispecific antibodies for immune cell retargeting against cancer. *Expert Opin. Biol. Ther.* 2022. 22: 965–982.
 - 42 Chen, W., Yang, F., Wang, C., Narula, J., Pascua, E., Ni, I., Ding, S., et al., One size does not fit all: navigating the multi-dimensional space to optimize T-cell engaging protein therapeutics. *MAbs* 2021. 13: 1871171.
 - 43 Haber, L., Olson, K., Kelly, M. P., Crawford, A., Dilillo, D. J., Tavaré, R., Ullman, E., et al. Generation of T-cell-redirecting bispecific antibodies with differentiated profiles of cytokine release and biodistribution by CD3 affinity tuning. *Sci Rep* 2021. 11: 14397.
 - 44 Liechti, T. and Roederer, M.. OMIP-060: 30-parameter flow cytometry panel to assess T cell effector functions and regulatory T cells. *Cytometry A.* 2019. 95: 1129–1134.
 - 45 Braakman, E., Sturm, E., Vijverberg, K., Van Krimpen, B. A., Gratama, J. W., Bolhuis, R. L. H., et al. Expression of CD45 isoforms by fresh and activated human $\gamma\delta$ T lymphocytes and natural killer cells. *Int. Immunol.* 1991. 3: 691–697.
 - 46 Wei, J., Montalvo-Ortiz, W., Yu, L., Krasco, A., Olson, K., Rizvi, S., Fiaschi, N., et al. CD22-targeted CD28 bispecific antibody enhances antitumor efficacy of onconectamab in refractory diffuse large B cell lymphoma models. *Sci. Transl. Med.* 2022. 14: eabn1082.
 - 47 Selvaggio, G., Parolo, S., Bora, P., Leonardelli, L., Harrold, J., Mehta, K., Rock, D. A., et al. Computational analysis of cytokine release following bispecific T-cell engager therapy: applications of a logic-based model. *Front Oncol.* 2022. 12: 818641.
 - 48 Ball, K., Dovedi, S. J., Vajjah, P. and Phipps, A. Strategies for clinical dose optimization of T cell-engaging therapies in oncology. *MAbs* 2023. 15: 2181016.
 - 49 Leclercq, G., Steinhoff, N., Haegel, H., De Marco, D., Bacac, M. and Klein, C., Novel strategies for the mitigation of cytokine release syndrome induced

- by T cell engaging therapies with a focus on the use of kinase inhibitors. *Oncoimmunology*. 2022. 11: 2083479.
- 50 Dang, K., Castello, G., Clarke, S. C., Li, Y., Balasubramani, A., Boudreau, A., Davison, L., et al. Attenuating CD3 affinity in a PSMAxCD3 bispecific antibody enables killing of prostate tumor cells with reduced cytokine release. *J Immunother Cancer* 2021. 9: e002488 .
- 51 Carrara, S C., Harwardt, J., Grzeschik, J., Hock, B. and Kolmar, H.. A tetrafunctional T-cell engaging antibody with built-in risk mitigation of cytokine release syndrome. *Front Immunol* 2022. 13: 1051875.
- 52 Kwant, K., Rocha, S., Stephenson, K., Dayao, M., Thothathri, S., Banzon, R., Aaron, W., et al., 867 TriTAC-XR is an extended-release T cell engager platform designed to minimize cytokine release syndrome by reducing Cmax in systemic circulation. *J. Immunother. Cancer* 2021. 9: A908–A908.
- 53 Mensurado, S., Blanco-Domínguez, R. and Silva-Santos, B.. The emerging roles of $\gamma\delta$ T cells in cancer immunotherapy. *Nat Rev Clin Oncol* 2023. 20: 178–191.
- 54 Johnson, D E., O'keefe, R A. and Grandis, J R.. Targeting the IL-6/JAK/STAT3 signalling axis in cancer. *Nat Rev Clin Oncol* 2018. 15: 234–248.
- 55 Philipp, N., Kazerani, M., Nicholls, A., Vick, B., Wulf, J., Straub, T., Scheurer, M., et al., T-cell exhaustion induced by continuous bispecific molecule exposure is ameliorated by treatment-free intervals. *Blood* 2022. 140: 1104–1118.
- 56 Lameris, R., Ruben, J M., Iglesias-Guimaraes, V., De Jong, M., Veth, M., Van De Bovenkamp, F S., De Weerd, I., et al., A bispecific T cell engager recruits both type 1 NKT and V γ 9V δ 2-T cells for the treatment of CD1d-expressing hematological malignancies. *Cell Rep Med* 2023. 4: 100961.
- 57 Xu, Y., Xiang, Z., Alnaggar, M., Kouakanou, L., Li, J., He, J., Yang, J., et al. Allogeneic V γ 9V δ 2 T-cell immunotherapy exhibits promising clinical safety and prolongs the survival of patients with late-stage lung or liver cancer. *Cell Mol Immunol*. 2021. 18: 427–439.

Abbreviations: **CEA:** tumor-associated antigen CEACAM5 · **CRS:** cytokine release syndrome · **FCS:** fetal calf serum · **ICB:** immune checkpoint blockade · **mAbs:** monoclonal antibodies · **MHC:** major histocompatibility complex · **PBMCs:** peripheral blood mononuclear cells · **PSMA:** prostate-specific membrane antigen · **rhIL-2:** recombinant human IL-2 · **RT:** room temperature · **TCEs:** T-cell engagers · **TCRs:** T-cell receptor chains · **TILs:** tumor-infiltrated T cells · **VHHs:** variable heavy domain of heavy chain-only antibody

Full correspondence: Dr. Emmanuelle Vigne, Sanofi, Large Molecule Research, Vitry-sur-Seine, F-94400, France
e-mail: Emmanuelle.Vigne@sanofi.com
Dr. Emmanuel Scotet, CRCl²NA, 8 quai Moncoussu, Nantes, F-44000, France
e-mail: Emmanuel.Scotet@univ-nantes.fr

Received: 13/9/2023
Revised: 23/4/2024
Accepted: 24/4/2024
Accepted article online: 20/5/2024